Interplay between Morphology and Compeition: Supplementary Information

Daniel Swartz, Hyunseok Lee, Mehran Kardar, and Kirill Korolev

July 2, 2023

1 Perturbative treatment of pushed waves

Here we explain in detail how to perform the perturbative treatment in the pushed wave case introduced in the main text. The starting point is the coupled FKPP and KPZ equations

$$\frac{\partial f}{\partial t} = s_1(f - f_0)f(1-f) + D_f\frac{\partial^2 f}{\partial x^2} + v_0\frac{\partial f}{\partial x}\frac{\partial h}{\partial x} \tag{1}$$

$$\frac{\partial h}{\partial t} = v_0 + \alpha f + D_h\frac{\partial^2 h}{\partial x^2} + \frac{v_0}{2}\left(\frac{\partial h}{\partial x}\right)^2. \tag{2}$$

We can remove the first term in Eq. (2) by shifting to a comoving frame and making the substitution $h \to h + v_0 t$. In this comoving frame, we are interested in travelling wave solutions which are fully described in a comoving coordinate $z = x - ut$ which moves with a speed u to be determined. For travelling wave solutions, Eqs. (1) and (2) take the form

$$-uf'(z) = s_1(f - f_0)f(1-f) + D_f f''(z) + v_0 f'(z)h'(z) \tag{3}$$

$$-uh'(z) = \alpha f(z) + D_h h''(z) + \frac{v_0}{2}h'(z)^2 \tag{4}$$

Further, we will consider the initial conditions $h(x, t = 0) = 0$ and $f(x, t = 0) = \theta(-x)$, corresponding to a half-space where the region $x < 0$ is occupied by mutant and $x > 0$ is occupied by wildtype. We will also analyze traveling waves for which the height field attains a constant slope σ as the mutant propagates into the wildtype. This is justified because for small values of $\alpha > 0$, the morphology is that of a composite bulge (see bottom of Fig. 2 in the main text) consisting of a central circular arc, and linear segments near the boundaries. This morphology is predicted by both the geometric theory and numerical solutions of the KPZ-FKPP equations. When $\alpha < 0$ the morphology is that of a v-shaped dent (Fig 2, main text) which also attains a constant slope. Eq. (4) immediately implies

$$-u\sigma = \alpha + \frac{v_0}{2}\sigma^2\,, \tag{5}$$

where we have used the fact $f \approx 1$ in region occupied by mutant. Eq. (5) provides a key relation between u and α and is exact.

We shall treat the nonlinear coupling $v_0 f'(z)h'(z)$ in Eq. (3) as as a perturbation. In the absence of this term, the solution to Eq. (1) is $f^{(0)}(z)$.

Substituting this zeroth order result in Eq. (4) leads to

$$-uh^{(1)\prime}(z) = \alpha f^{(0)}(z) + D_h h^{(1)\prime\prime}(z) + \frac{v_0}{2}h^{(1)\prime}(z)^2\,. \tag{6}$$

Substituting the resulting $h^{(1)}$ into Eq. (3) leads to

$$-uf'(z) = R(f(z)) + D_f f''(z) + v_0 f'(z)h^{(1)\prime}(z)\,. \tag{7}$$

Here $R(f) = s_1(f - f_0)f(1 - f)$ is the local growth function, but we write it in this form to stress that this calculation is generic. We now demonstrate how to solve Eqn. (7) perturbatively. Following the approach discussed in [4, 6, 5, 7], we expand the terms in Eq. (7) as $f = f^{(0)} + \delta f$ and $u = u_0 + \delta u$ and neglect terms of order $O(\delta f^2, \delta u^2, \delta f \delta u)$. We then have

$$-\delta u f^{(0)\prime} - u_0 \delta f' \approx R'(f^{(0)})\delta f + D_f \delta f'' + v_0 h^{(1)\prime} f^{(0)\prime}, \tag{8}$$

where the prime on the growth function R denotes a derivative with respect to its argument. We have neglected the term $h^{(1)\prime}\delta f'$, which is second order in the perturbation in the small slope limit. We can collect all the terms containing the correction to the profile shape δf to find

$$-\delta u f^{(0)\prime} - v_0 f^{(0)\prime} h^{(1)\prime} = u_0 \delta f' + R'(f^{(0)})\delta f + D_f \delta f'' = \mathcal{L}\delta f. \tag{9}$$

The RHS involves a linear operator $\mathcal{L}$ which quantifies the "restoring force" due to perturbations in the front shape.

Note that our last equation has two unknowns, so we need an additional condition to solve it. This extra condition delineates what changes in the dynamics are encoded in δu and what changes are encoded in δf. Since δu is the change in the velocity, it should account for the changes in the translational motion of the front, while δf should include only changes in front shape and not its motion. Thus, δf should be orthogonal to the translation of the unperturbed front. This idea can be implemented mathematically as follows.

Recall that the unperturbed profile shape solves $-u_0 f^{(0)\prime} = R(f^{(0)}) + D_f f^{(0)\prime\prime}$, then differentiation by z immediately yields that $\mathcal{L}f^{(0)\prime} = 0$ demonstrating that $\mathcal{L}$ (and its adjoint $\mathcal{L}^\dagger$) has a zero eigenvector. We can find this zero eigenvector for the adjoint $L(z)$ by solving

$$\mathcal{L}^\dagger L = 0.$$

Using the ansatz $L(z) = \nu(z) f^{(0)\prime}(z)$, we find the following relation for the unknown function $\nu(z)$.

$$\left(-2u_0\nu + 2D_f\nu'\right) f^{(0)\prime\prime} + \left(-u_0\nu' + D_f\nu''\right) f^{(0)\prime} = 0 \tag{10}$$

Which is solved for $\nu(z) = e^{u_0 z/D_f}$. Multiplying both sides of our expanded Eq. (9) by $L(z)$ and integrating over all z, the RHS vanishes by the eigenvector property of L, and we find a closed form expression for the correction to the invasion velocity

$$\delta u = -v_0 \frac{\int_{-\infty}^{\infty} (f^{(0)\prime})^2 e^{u_0 z/D_f} h^{(1)\prime} dz}{\int_{-\infty}^{\infty} (f^{(0)\prime})^2 e^{u_0 z/D_f} dz}. \tag{11}$$

We again stress that this correction was found without referencing the exact form of the growth function R or the zeroth order solution $f^{(0)}$. Given a result for $h^{(1)}$, as discussed next, the ratio of integrals can be evaluated numerically to give the numerical value of the velocity correction and κ in the main text.

2 The Cole-Hopf transformation

For the pushed waves considered in the main text with $s(f) = s_1(f - f_0)$, the unperturbed profile shape is

$$f^{(0)}(z) = \frac{1}{1 + e^{z/a}}, \tag{12}$$

where $a = \sqrt{\frac{2D_f}{s_1}}$ and the uncoupled velocity is $u_0 = \sqrt{\frac{s_1 D_f}{2}}(1 - 2f_0)$.With this profile shape $f^{(0)}(z)$, Eq. (6) can be solved exactly with the use of a Cole-Hopf transformation, $w \equiv \exp\left[(v_0 h/(2D_h)\right]$, where we substitute $h^{(1)\prime}(z) = \frac{2D_h}{v_0} w'(z)/w(z)$. Equation (6) then simplifies to

$$w'' + \frac{u}{D_h} w' + \frac{1}{1 + e^{z/a}} \frac{\alpha v_0}{2D_h^2} w = 0\,. \tag{13}$$

This simplified equation has two solutions w_1 and w_2 given by

$$w_1 = e^{-\frac{u+\sqrt{u^2-2\alpha v_0}}{2D_h}z}\,{}_2F_1(-\frac{u+\sqrt{u^2-2\alpha v_0}}{2D_h a^{-1}}, \frac{u-\sqrt{u^2-2\alpha v_0}}{2D_h a^{-1}}, 1-2\frac{\sqrt{u^2-2\alpha v_0}}{2D_h a^{-1}}, -e^{z/a}),$$
$$w_2 = e^{\frac{u-\sqrt{u^2-2\alpha v_0}}{2D_h}z}\,{}_2F_1(-\frac{u-\sqrt{u^2-2\alpha v_0}}{2D_h a^{-1}}, \frac{u+\sqrt{u^2-2\alpha v_0}}{2D_h a^{-1}}, 1+2\frac{\sqrt{u^2-2\alpha v_0}}{2D_h a^{-1}}, -e^{z/a}),$$

where ${}_2F_1$ is a hypergeometric function. The general solution to Eq. (13) is then a linear combination of w_1 and w_2. When mapping these solutions back onto the height field h, only w_2 satisfies the essential boundary condition that $h^{(1)\prime} \to 0$ as $\alpha \to 0$. This is most immediately seen using the fact that the ${}_2F_1$ function is unity when its first argument vanishes. For this reason we throw out w_1. The slope of the height field is then

$$h^{(1)\prime} = \frac{-u+\sqrt{u^2-2\alpha v_0}}{v_0} + e^{z/a}\frac{\alpha v_0^2 a/D_h}{1+a\sqrt{u^2-2\alpha v_0}/D_h}\frac{{}_2F_1(1-\frac{u-\sqrt{u^2-2\alpha v_0}}{2D_h a^{-1}}, 1+\frac{u+\sqrt{u^2-2\alpha v_0}}{2D_h a^{-1}}, 2+2\frac{\sqrt{u^2-2\alpha v_0}}{2D_h a^{-1}}, -e^{z/a})}{{}_2F_1(-\frac{u-\sqrt{u^2-2\alpha v_0}}{2D_h a^{-1}}, \frac{u+\sqrt{u^2-2\alpha v_0}}{2D_h a^{-1}}, 1+2\frac{\sqrt{u^2-2\alpha v_0}}{2D_h a^{-1}}, -e^{z/a})} \quad . \tag{14}$$

The expression for $h^{(1)\prime}$ is formally exact, and can be substituted into Eq. (11) to give a nonlinear equation for u which can then be solved numerically. This is a complex numerical task which can be circumvented in the limit $\alpha \to 0$ which is identified with a small slope expansion.

2.1 Linear approximation for small α

For small α, a direct expansion of Eq. (14) yields a simplified form of $h^{(1)\prime}$,

$$h^{(1)\prime}(z) = -\frac{\alpha}{u}\,{}_2F_1\left(1, \frac{au}{D_h}, 1+\frac{au}{D_h}, -e^{z/a}\right) + O(\alpha^2). \tag{15}$$

This expression is also obtainable by solving Eq. (6) while ignoring the quadratic term, which is anticipated to be $O(\alpha^2)$. Following the methodology of the expansion of Eq. (7), we decompose $u = u_0 + \delta u$. As the original equations are decoupled for $\alpha = 0$, δu must be $O(\alpha)$ and thus can be neglected in Eq. (15). The approximate form of $h^{(1)\prime}$ is then further simplified with the use of Eq. (5) to replace α with σ (to leading order). The final expression for $h^{(1)\prime}$ is

$$h^{(1)\prime}(z) \approx \sigma\ {}_2F_1\left(1, \frac{au_0}{D_h}, 1+\frac{au_0}{D_h}, -e^{z/a}\right). \tag{16}$$

This can now be immediately substituted into Eq. (11)

$$\delta u \approx -v_0\sigma \underbrace{\frac{\int_{-\infty}^{\infty}(f^{(0)\prime})^2 e^{u_0 z/D_f}\,{}_2F_1\left(1, \frac{au_0}{D_h}, 1+\frac{au_0}{D_h}, -e^{z/a}\right)dz}{\int_{-\infty}^{\infty}(f^{(0)\prime})^2 e^{u_0 z/D_f}dz}}_{\kappa} \tag{17}$$

and the integrals can be calculated numerically to give a closed-form solution for the correction to the invasion velocity δu. The underlined piece is the response coefficient κ reported in Figs. (3) and (4) in the main text.

2.2 The geometric limit

A further limit can be taken, which provides the advantage of simplifying the result of integrating Eq. (11). We call this limit the "geometric limit" which is achieved by setting $D_h = 0$. Physically, the geometric limit corresponds to the case where the height field h no longer relaxes due to surface rearrangement and instead only advances along the direction of the unit normal. The geometric limit also corresponds to the "equal

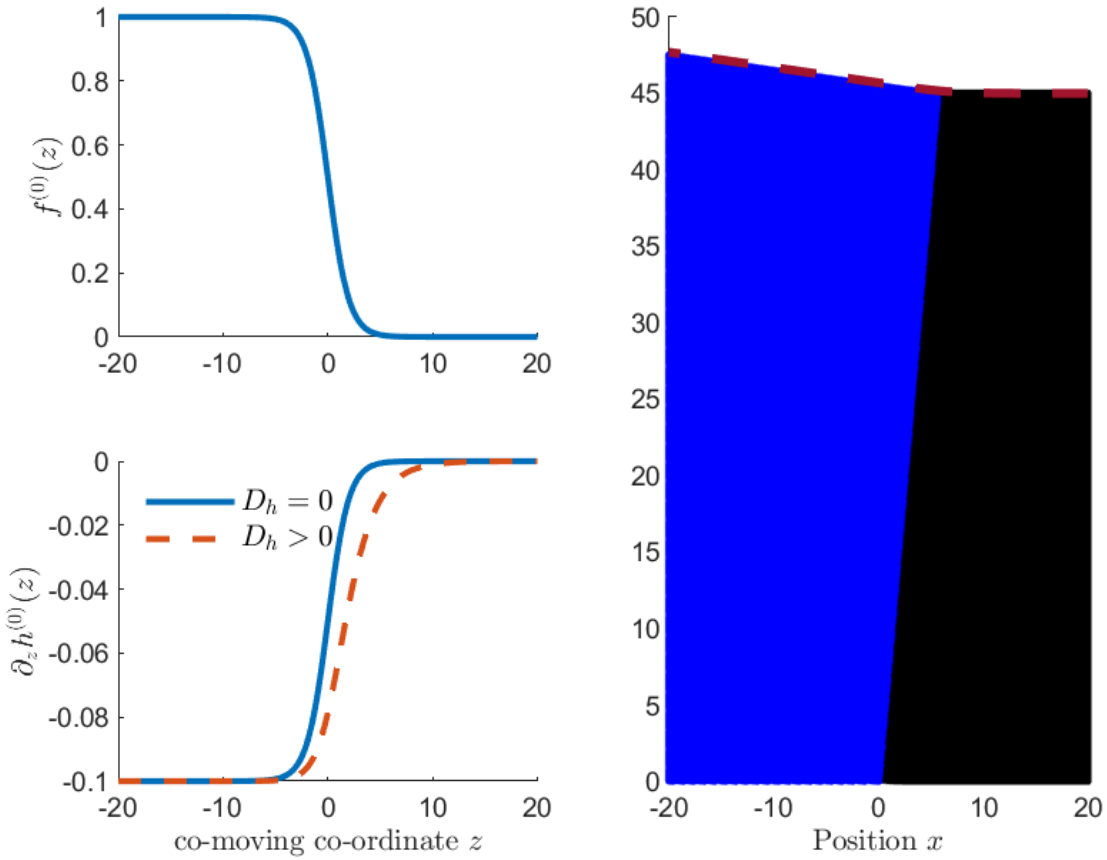

Figure 1: Sample showing the solution to the travelling wave problem in the geometric limit. (Top Left) Plot showing the zeroth order mutant frequency wave form (12) as a function of the co-moving co-ordinate $z = x - ut$. (Bottom Left) The solid line is the solution to Eq. (6) in the geometric limit and for small α from Eq. (19). The dashed line is the solution with surface relaxation, again in the small α limit, as given by Eq. (15). The right plot is the perturbative solution for the morphology in the geometric limit. The height field is found by integrating Eq. (19) with the zeroth order frequency profile described by Eq. (12). This surface expands along its unit normal, and the speed of invasion is given by Eq. (20). The parameters are $\alpha = 0.1, v_0 = 10, u_0 = 1, \kappa = 0.25$ ($f_0 = 0$). The dashed lines in the lower-left and right panels are for $D_h = 2$. We note that even though a different value of D_h will change the prediction for the invasion speed u, the first order morphology is independent of this difference as it only depends on the bare speed u_0 so these morphologies can be directly compared.

time" approach discussed in previous works [3, 2]. Such a limit allows for the case of cusps and sharp corners, in the height field. It is simplest to proceed from Eq. (6), with $D_h = 0$. The resulting quadratic equation is readily solved to give

$$h^{(1)\prime}(z) = \frac{-u \pm \sqrt{u^2 - 2\alpha v_0 f^{(0)}(z)}}{v_0}. \tag{18}$$

Upon substitution into Eq. (11), we again encountered a nonlinear equation for u. We further simplify it again expanding in small α, where the height profile is now

$$h^{(1)\prime}(z) \approx \sigma f^{(0)}(z). \tag{19}$$

We have again used Eq. (5) to remove α. Eq. (11) can now be integrated exactly, and we find

$$\delta u = -v_0\Big(\frac{1}{4} + \frac{f_0}{2}\Big)\sigma, \tag{20}$$

a rather simple expression for the correction to the invasion velocity. In the context of Eq. (17) and Fig. 4 in the main text, the geometric limit has $\kappa = \frac{1}{4} + \frac{f_0}{2}$.

The $D_h = 0$ limit is singular, and leads to jagged profiles that are smoothed for $D_h > 0$. However this form of κ makes explicitly clear that the correction to the wave-speed should vanish as $f_0 \to -1/2$. This value of f_0 is known to correspond with the onset of pulled waves [1, 8]. This feature is general, the $D_h > 0$ correction also vanishes for $f_0 \to -1/2$ which can be verified by showing the denominator of Eq. (11) diverges while the numerator remains finite.

3 Transition from composite bulge to circular arc

In our numerical simulations, the invasion velocity u switches from being described by our perturbative analysis (Eq. (17)) to the speed of a circular arc. This transition occurs at a critical value of the expansion speed difference α_c, and suggests that the assumption of a constant slope σ near the mutant-wildtype boundary made in our perturbative calculation are no longer valid for $\alpha > \alpha_c$. In this section, we show that the composite bulge morphology is unstable for large α and must become a circular arc morphology in the long time limit. This observation explains why we see the invasion speed collapse onto that of a circular arc in both the pulled and pushed wave dynamics (see Figs. 3 and 4 as well as Figs. 2 and 3 in the main text).

The composite bulge morphology is shown in Fig. 5, and consists of a central circular arc with sloped edges of slope σ. The boundary between the circular arc and composite bulge section advances with speed u_{boundary}, and this morphology will persist only if the speed of invasion u exceeds the speed of the boundary, that is $u > u_{\text{boundary}}$ is required for the composite bulge to be stable to morphological invasion. The location of the circle-slope boundary can be found by demanding that $\partial h/\partial x$ be continuous, to first order one immediately finds

$$-\frac{x_{\text{boundary}}}{(v_0 + \alpha)t} = \sigma \to u_{\text{boundary}} = -v_0\sigma + O(\alpha^2). \tag{21}$$

We have explicitly neglected terms like $\alpha\sigma$ as σ is anticipated to be of order α. The speed of advance of the mutant is the solution to the system of equations

$$u = u_0 - \kappa v_0 \sigma \tag{22}$$

$$-u\sigma = \alpha + \frac{v_0}{2}\sigma^2. \tag{23}$$

We can find the transition point where u_{boundary} exceeds the invasion speed u by substituting $u = u_{\text{boundary}} = -v_0\sigma$ into the above. Solving this system, one immediately finds that the boundary and invasion velocity are equal when

$$\alpha = \frac{u_0^2}{2v_0(1-\kappa)^2} \equiv \alpha_c. \tag{24}$$

When $\alpha > u_0^2/2v_0(1-\kappa)^2$, the composite bulge cannot be the long term solution of our equations as it will eventually be subsumed by its central circular arc. To check that this value of the growth rate difference α

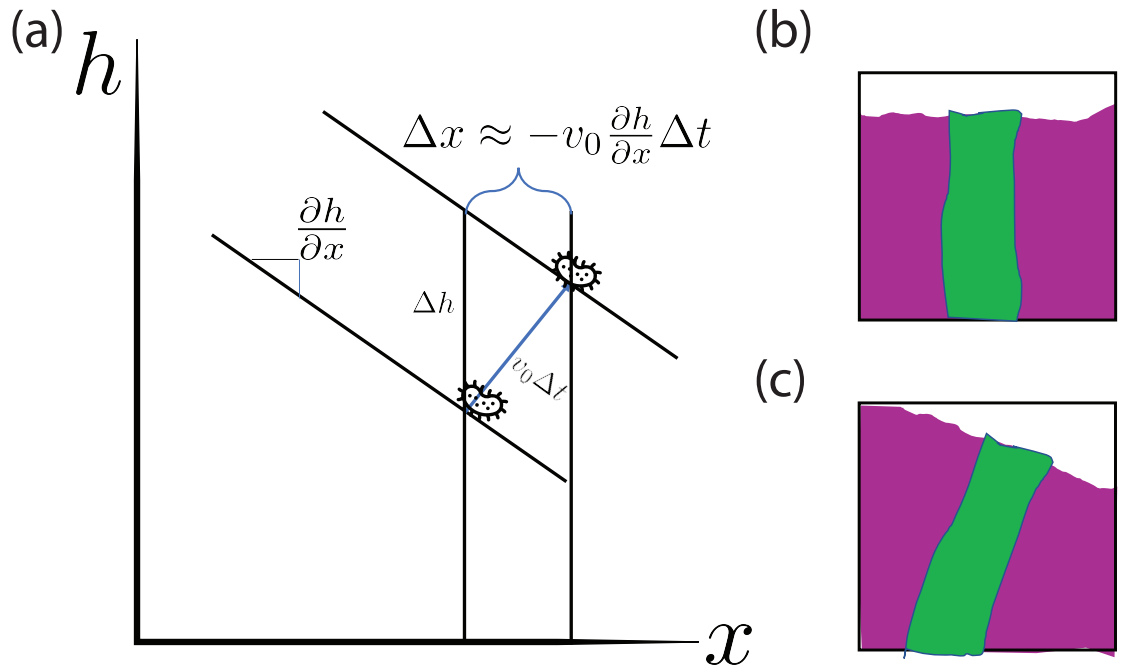

Figure 2: Cartoon demonstrating the origin of the advective term in Eq. (1). In (a), a simple geometric calculation shows that an individual on the front of a population will have children displaced by an amount $\Delta x \approx v_0 \partial h/\partial x \Delta t$, which defines the advection velocity due to growing on a tilted surface. In (b) and (c), we sketch how this advection manifests at the level of sector growth. In (b), the leading surface is flat and as such the sector stays centered as it grows. By tilting the leading surface as in (c) the region occupied by the green species translates horizontally.

does indeed correspond to the transition to a circular arc, we can plug $\alpha = u_0^2/2v_0(1-\kappa)^2$ in to Eqs. (22) and (23) and solving for u we find

$$u = \frac{u_0}{1-\kappa} = \sqrt{2\alpha v_0} \tag{25}$$

matching the speed of a circular arc as expected. This demonstrates that the transition between the composite bulge and circular arc occurs when the velocities predicted by each morphology are equal, and this transition point coincides with the parameter values where the composite bulge morphology is an unstable solution of our equations.

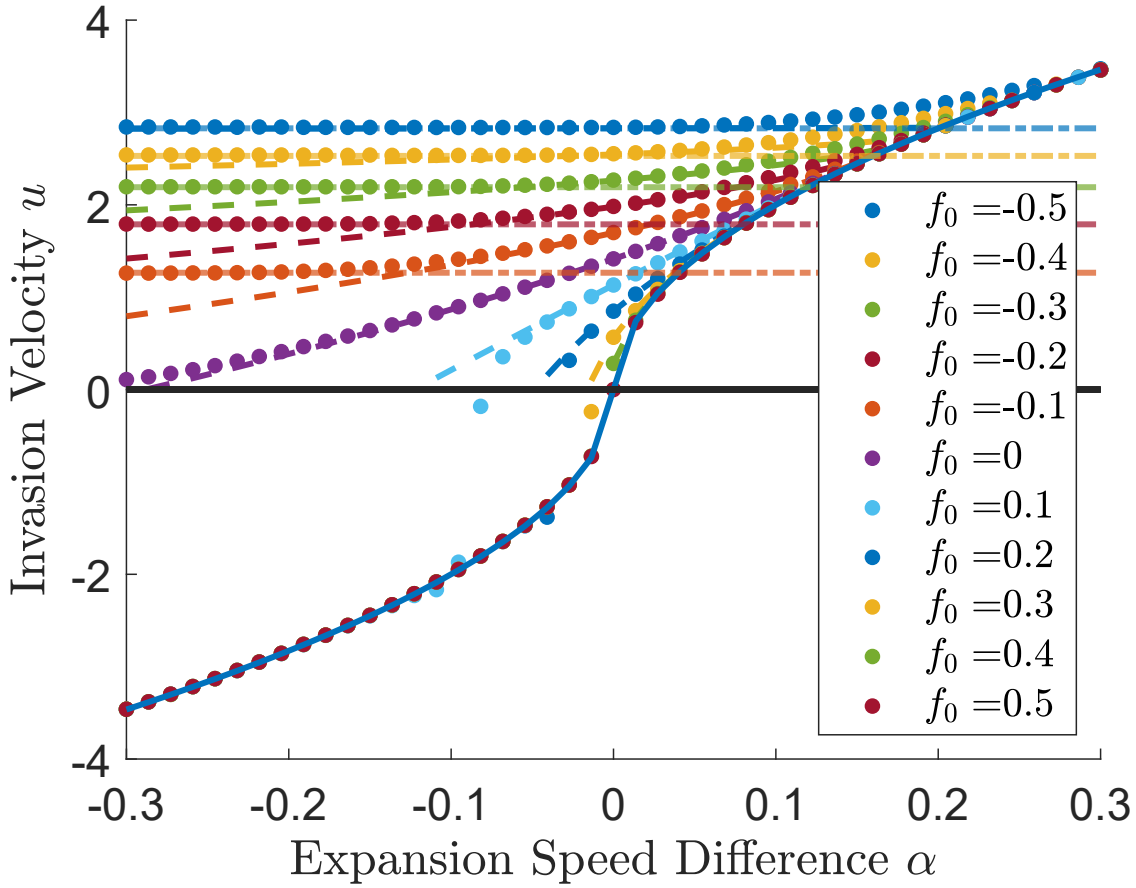

Figure 3: Numerical results measuring the invasion velocity u as a function of the expansion speed difference α for a range of values of f_0. The dots are the result of numerical simulation, while the dashed lines are the analytic predictions from our perturbative calculation. The dash-dotted lines show the asymptotic velocity $2\sqrt{-f_0 s_1 D_f}$, consistent with a linearized Eq. (1) when $f_0 < 0$. While all the data are well described by the perturbative calculation for small $|\alpha|$, it appears that when $f_0 < 0$, the invasion velocity approaches some constant as α becomes increasingly negative. All data for $f_0 > 0$ indeed collapse onto the velocity of a leftbound circular arc. Both circular arc velocities shown by the solid blue line for comparison. Parameters are $s_1 = 4, D_f = D_h = 1, v_0 = 20$.

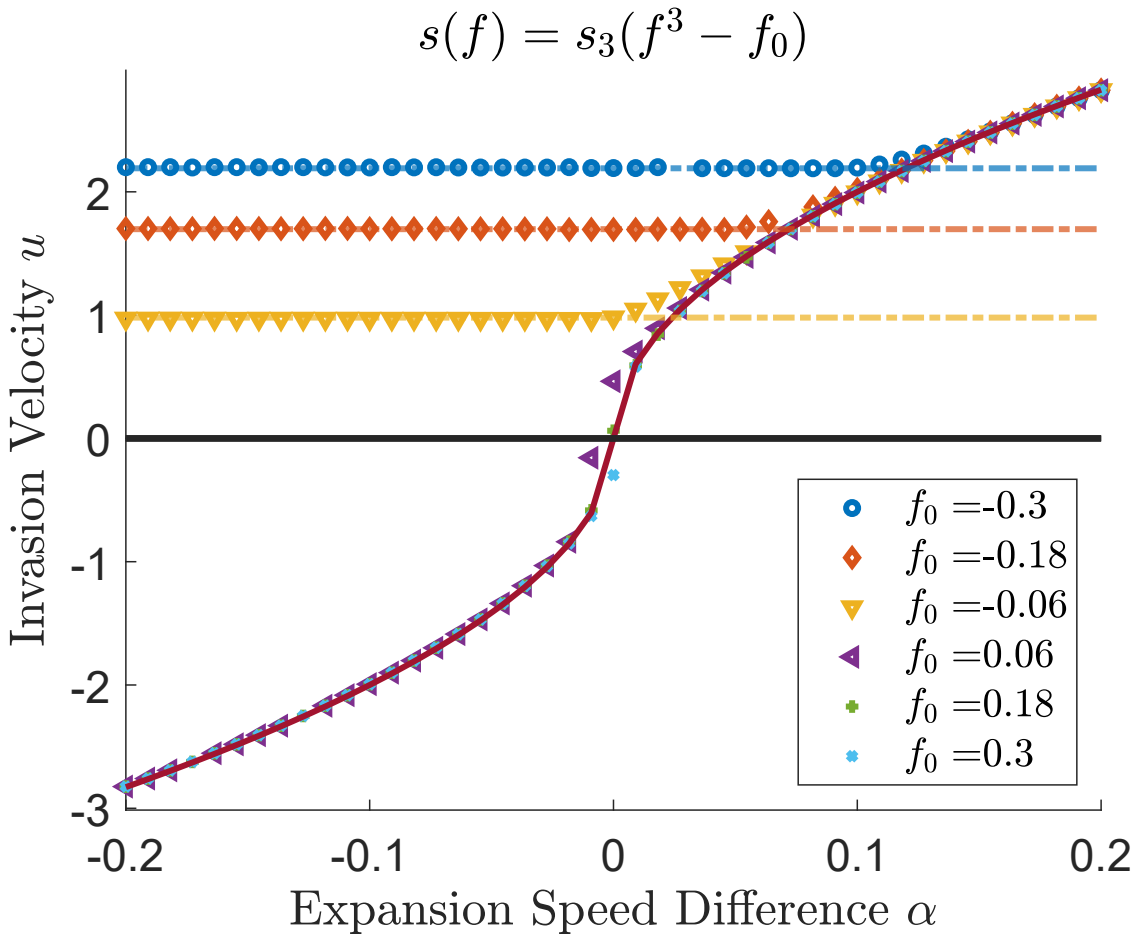

Figure 4: Numerical results measuring the invasion velocity u as a function of the expansion speed difference α for a *different* selection coefficient function $s(f) = s_3(f^3 - f_0)$. The red solid red line shows the two way circular arc velocity $u = \text{sign}(\alpha)\sqrt{2|\alpha|v_0}$. The dash-dotted lines show the asymptotic velocity $2\sqrt{-f_0 s_1 D_f}$, consistent with a linearized Eq. (1) when $f_0 < 0$. We see that even with a different fitness function from that treated in the main text, the invasion velocity still varies nontrivially with the expansion speed difference α and the main qualitative features of this variation are reproduced. When α is large and positive all the data collapse onto the speed of a rightward moving circular arc. When α is sufficiently negative the data are either consistent with that of the linearized equations for $f_0 < 0$ or a leftward moving circular arc for $f_0 > 0$.

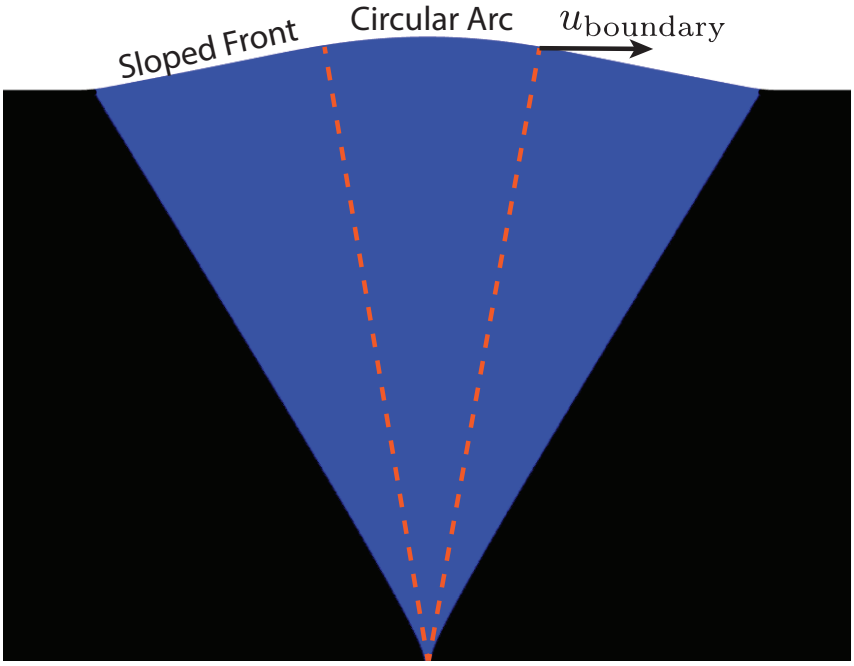

Figure 5: Sketch of a comosite bulge morphology, which has a central circular arc and sloped edges with slope σ. The boundary between the circular and sloped sections advances with speed u_{boundary}, and the composite bulge morphology can only persist as $t \to \infty$ when u_{boundary} is less than the mutant invasion speed u.

References

[1] Gabriel Birzu, Oskar Hallatschek, and Kirill S Korolev. Fluctuations uncover a distinct class of traveling waves. *Proceedings of the National Academy of Sciences*, 115(16):E3645–E3654, 2018.

[2] Oskar Hallatschek and David R Nelson. Life at the front of an expanding population. *Evolution: International Journal of Organic Evolution*, 64(1):193–206, 2010.

[3] Kirill S Korolev, Melanie JI Müller, Nilay Karahan, Andrew W Murray, Oskar Hallatschek, and David R Nelson. Selective sweeps in growing microbial colonies. *Physical biology*, 9(2):026008, 2012.

[4] Baruch Meerson, Pavel V Sasorov, and Yitzhak Kaplan. Velocity fluctuations of population fronts propagating into metastable states. *Physical Review E*, 84(1):011147, 2011.

[5] AS Mikhailov, L Schimansky-Geier, and W Ebeling. Stochastic motion of the propagating front in bistable media. *Physics Letters A*, 96(9):453–456, 1983.

[6] GC Paquette, Lin-Yuan Chen, Nigel Goldenfeld, and Y Oono. Structural stability and renormalization group for propagating fronts. *Physical review letters*, 72(1):76, 1994.

[7] Andrea Rocco, Jaume Casademunt, Ute Ebert, and Wim van Saarloos. Diffusion coefficient of propagating fronts with multiplicative noise. *Physical Review E*, 65(1):012102, 2001.

[8] Wim Van Saarloos. Front propagation into unstable states. *Physics reports*, 386(2-6):29–222, 2003.